SUPPLEMENTARY MATERIALS AND METHODS

Sequence alignments

Human protein sequences were obtained from UniProtKB Release 13.0 (The UniProt Consortium, 2010). Non-human protein sequences were downloaded from OrthoMCL-DB Version 3 (*1*), and the OrthoMCL server was used to assign human sequences to ortholog groups. To construct sets of orthologs unique to each human protein, in-house scripts were used first to identify non-human orthologs from selected species that belonged to the same ortholog group as the human protein. When multiple paralogs from the same species were present within the same group, the bit score generated by pairwise BLASTP (BLAST2 Version 2.2.20) for each paralog and the human protein was used to select only the paralog most similar to the human sequence. The sequences within each of the final ortholog groups were aligned using MUSCLE 3.70 (*2*), and in-house scripts were used to identify columns in the alignments that matched the observed phosphorylation sites in the human proteins. Each potential phosphorylation site contained in a ModSite was investigated independently. R (R Development Core Team, 2009) was used to perform hierarchical clustering of phosphorylation site data by Euclidean distance. Abbreviations for species are the following *Homo sapiens* (hsap), *Pan troglodytes* (ptro), *Canis lupus* (clup), *Mus musculus* (mmus), *Rattus norvegicus* (rnor), *Monodelphis domestica* (mdom), *Ornithorhynchus anatinus* (oana), *Gallus gallus* (ggal), *Tetraodon nigroviridis* (tnig), *Takifugu rubripes* (trub), *Danio rerio* (drer), *Ciona intestinalis* (cint), *Bombyx mori* (bmor), *Anopheles gambiae* (agam), *Drosophila melanogaster* (dmel), *Apis mellifera* (agam), *Brugia malayi* (bmaa), *Caenorhabditis briggsae* (cbri), *Caenorhabditis elegans* (cele), *Schistosoma mansoni* (sman), *Nematostella vectensis* (nvec), *Neurospora crassa* (ncra), *Schizosaccharomyces pombe* (spom), *Candida glabrata* (cgla), and *Saccharomyces cerevisiae* (scer).

The programs PSIPRED Version 2.61 (*3*) and DISOPRED Version 2.4 (*4*) were used to predict regions of secondary structure and order versus disorder, respectively, for human protein sequences.

Pathway analysis

Annotation of spindle, centrosome and centromere/kinetochore proteins was based on curated literature references, UniProt citations, and the Ingenuity software. Information on known kinase substrates were extracted from NCI Pathways (http://pid.nci.nih.gov/) as well as literature resources. Overall connectivity of identified phosphoproteins was determined using STRING (*5*). Highly connective subnetworks in the STRING network were identified using MCODE plug-in into Cytoscape (*6*).

A

Spindle phenotypes:

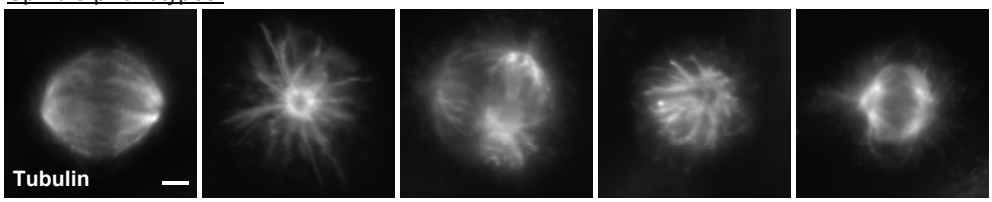

	bipolar	monopolar	multipolar	aberrant	pseudo-bipolar
control	94.1%	0.0%	5.9%	0.0%	0.0%
MLN8054 0.25μM	60.9%	1.6%	6.3%	31.3%	0.0%
MLN8054 1μM	14.8%	2.1%	14.8%	45.5%	22.8%
MLN8054 5μM	0.0%	1.6%	22.5%	49.6%	26.4%
BI2536 0.1μm	11.6%	88.4%	0.0%	0.0%	0.0%
AZD1152 1μm	37.5%	0.0%	10.8%	51.7%	0.0%
ZM447439 5μM	33.1%	1.8%	10.1%	55.0%	0.0%

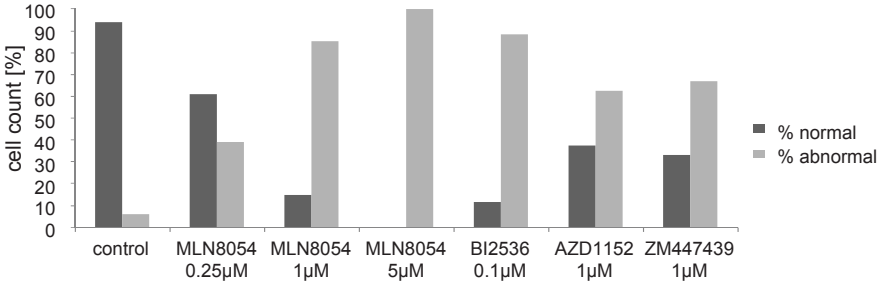

B

Chromosome phenotypes:

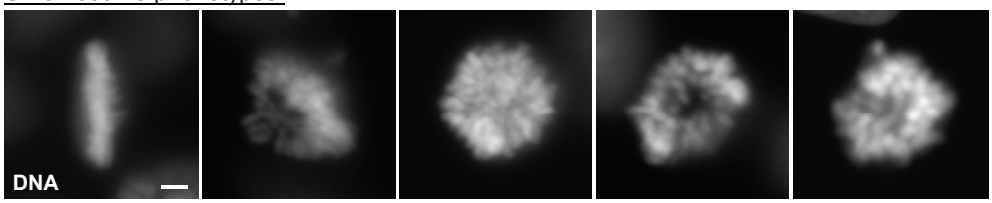

	aligned	misaligned	rosette-like	halo-like	monopolar
control	93.1%	6.9%	0.0%	0.0%	0.0%
MLN8054 0.25μM	46.1%	10.2%	42.2%	0.0%	1.6%
MLN8054 1μM	20.6%	21.7%	55.6%	0.0%	2.1%
MLN8054 5μM	10.9%	43.4%	44.2%	0.0%	1.6%
BI2536 0.1μm	5.8%	5.8%	0.0%	0.0%	88.4%
AZD1152 1μm	17.5%	35.8%	13.3%	33.3%	0.0%
ZM447439 5μM	18.3%	37.3%	21.3%	21.3%	1.8%

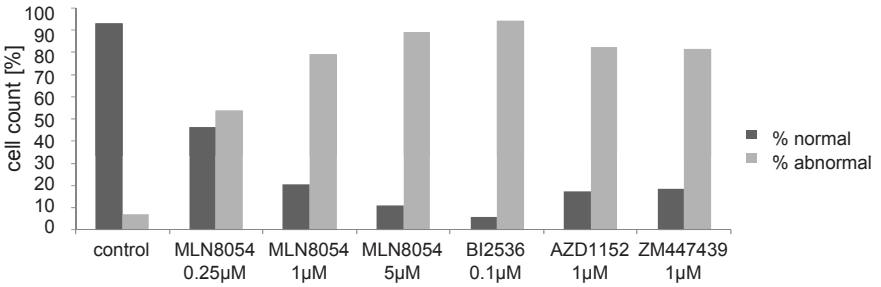

Fig. S1. Spindle and chromosome morphology of inhibitor-treated HeLa cells. (**A**) Spindle phenotypes of inhibitor-treated HeLa cells in mitosis were scored on the basis of the number of spindle poles as observed by tubulin stain (one- monopolar, two- bipolar, more than two-multipolar, not determinable- aberrant). Cells were categorized as pseudo-bipolar if they appeared to have two poles, but displayed a compressed spindle with an increased number of astral microtubules emanating from the poles. Bar diagram depicting percentage of cells with normal and abnormal spindle morphologies under different conditions of inhibitor treatment. Monopolar, multipolar, pseudo-bipolar, and aberrant spindles were scored as abnormal, whereas bipolar spindles were scored as normal. At least 100 cells were scored for each treatment (control or inhibitor). (**B**) Chromosome phenotypes of inhibitor-treated HeLa cells in mitosis as observed by Hoechst and CREST staining. CREST is human serum containing antibodies that react with kinetochore-localized proteins. Cells displaying a monopolar spindle were scored as having a monopolar chromosome phenotype. Bar diagram depicting percentage of cells with normal and abnormal chromosome morphology. Misaligned, rosette-like, halo-like, and monopolar chromosome morphology were scored as abnormal, whereas aligned chromosomes was scored as normal. At least 100 cells were scored for each treatment (control or inhibitor).

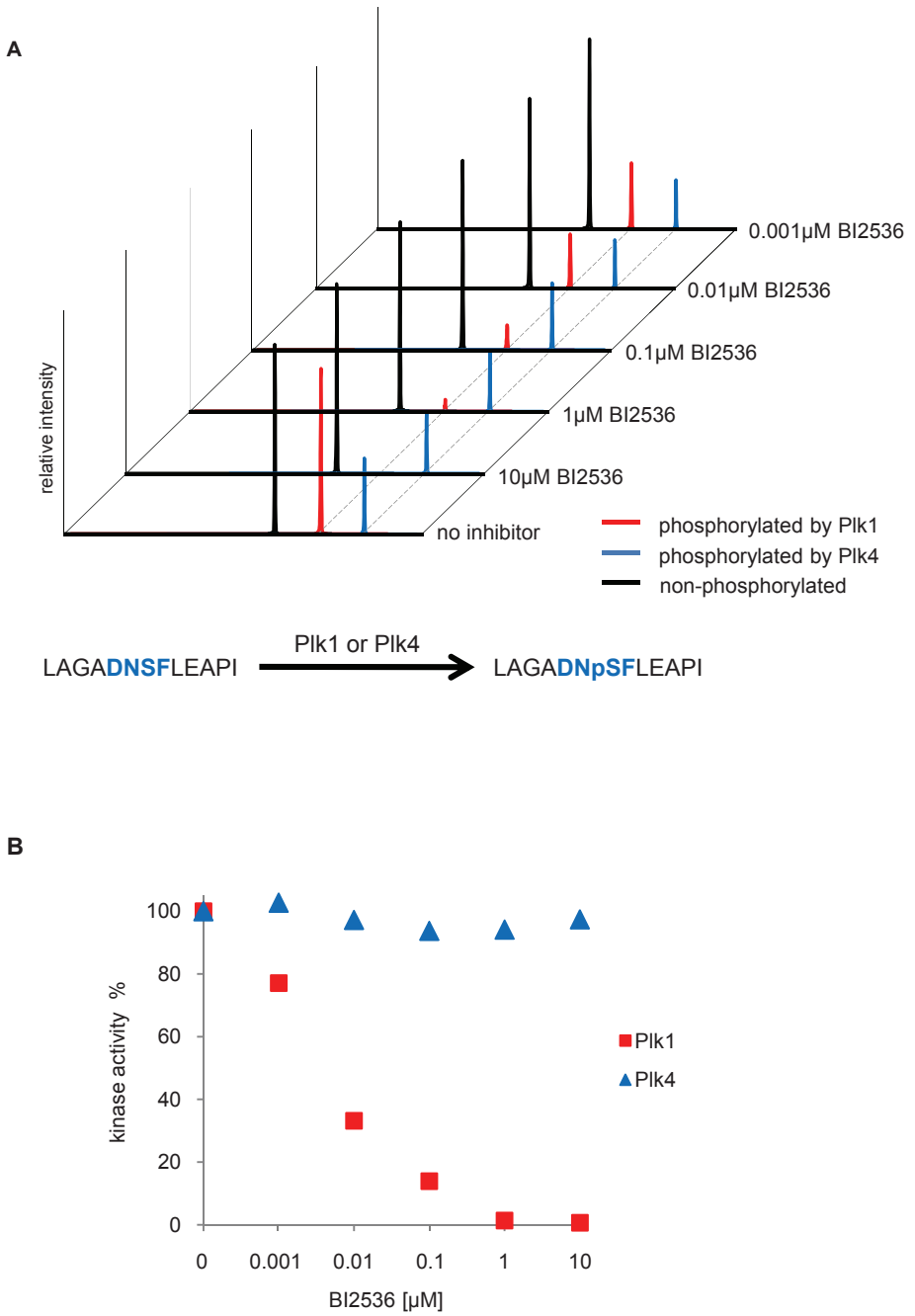

Fig. S2. Plk1 and Plk4 inhibition by BI2536. (**A**) MS1 intensity trace of the phosphorylated and nonphosphorylated peptide LAGADNSFLEAPI from Plk1 and Plk4 in vitro kinase reactions at different concentrations of BI2536. (**B**) Diagram depicting relative kinase activity as measured in the in vitro kinase reactions shown in panel A. Whereas Plk1 is inhibited by low concentrations of BI2536, Plk4 activity does not change at any concentration of BI2536.

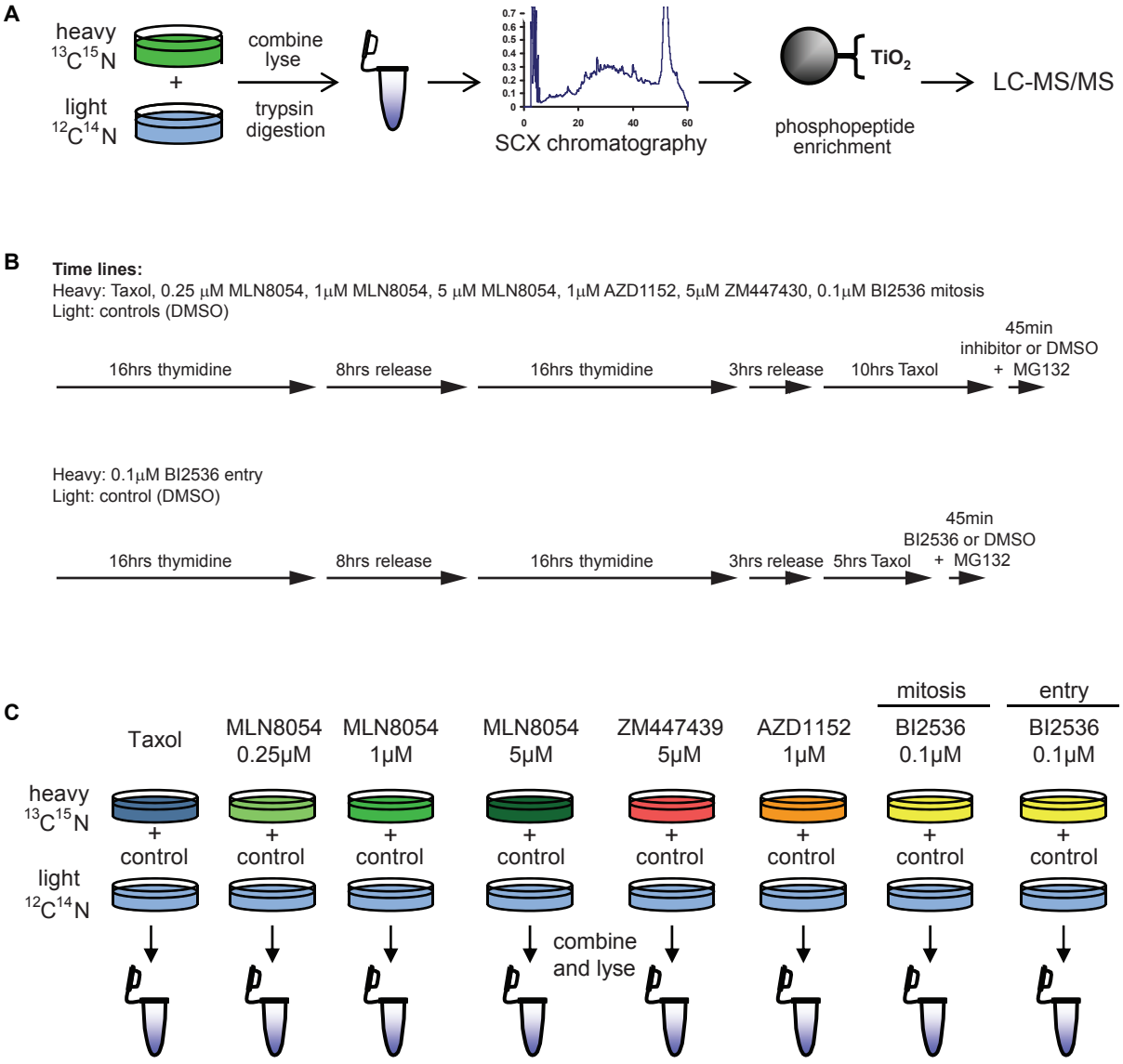

Fig. S3 Experimental setup and schematic of time line of HeLa cell synchronization. (**A**) Scheme of SILAC strategy to identify mitotic kinase-specific substrates of Aurora A, B, and Plk. HeLa cells labeled with “heavy” arginine and lysine were arrested in mitosis with Taxol and treated with kinase inhibitor and MG132. Light cells were arrested in mitosis with Taxol and MG132 and control-treated with DMSO. Afterwards, cells were counted, mixed, lysed, and digested with trypsin. Peptides were separated by SCX chromatography, and phosphopeptides were isolated from each fraction with titanium dioxide microspheres and analyzed by LC-MS/MS. (**B**) Time line of HeLa cell synchronization for the different inhibitor and control conditions. (**C**) Experimental setup for inhibitor SILAC experiments.

A

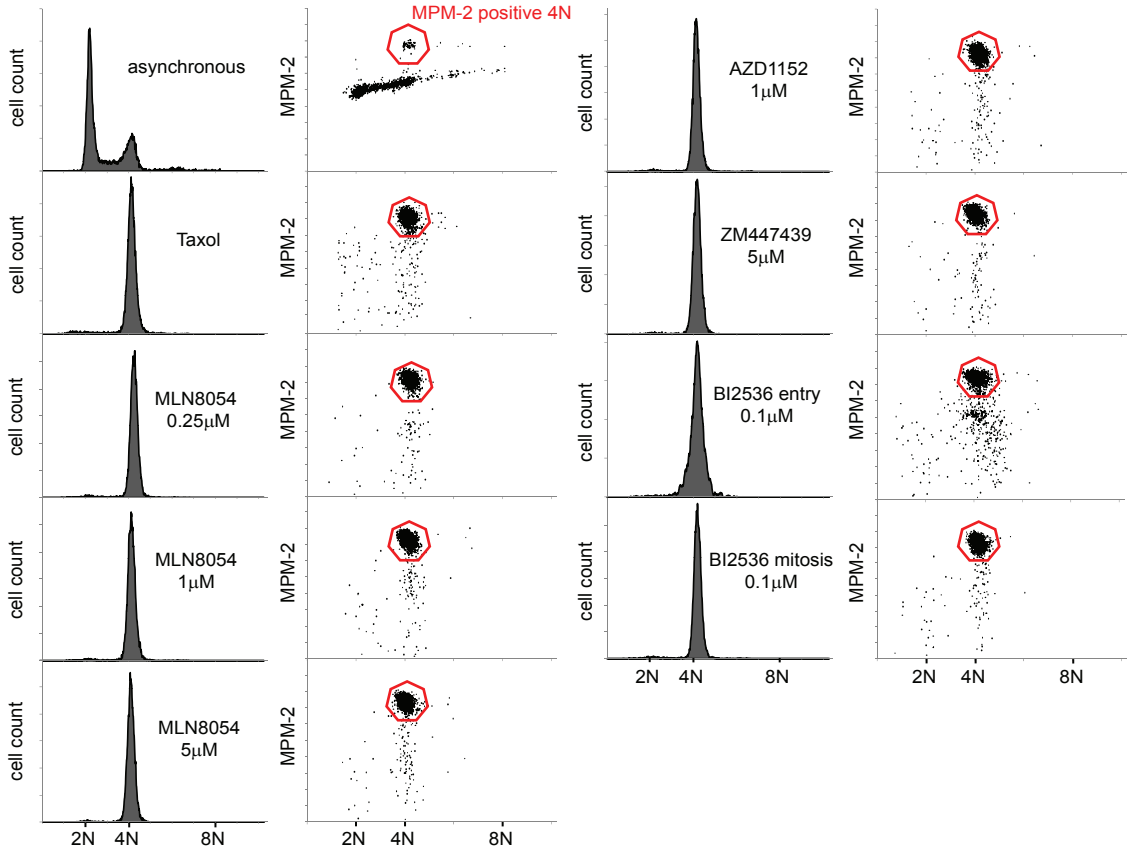

B

	asynchronous	Taxol	MLN8054 0.25μM	MLN8054 1μM	MLN8054 5μM	AZD1152 1μM	ZM447439 5μM	BI2536 0.1μM mitosis	BI2536 0.1μM entry
G1	61.9%	2.3%	2.7%	2.4%	2.7%	2.5%	2.3%	2.7%	2.7%
G2/M	18.7%	94.8%	95.9%	96.6%	95.8%	96.4%	96.6%	96.1%	93.2%
MPM-2	3.6%	89.3%	91.8%	92.6%	90.9%	91.8%	90.9%	92.0%	72.2%
pS10 H3	4.5%	88.4%	88.9%	89.1%	na	na	na	90.2%	74.1%

Fig. S4. Flow cytometry analysis of inhibitor-treated HeLa cells. (**A**) Flow cytometry profiles of DNA content and MPM-2 staining, which stains mitotic cells, of asynchronous, Taxol-arrested, and Taxol + inhibitor-treated HeLa cells. (**B**) Table indicating the percentage of cells in G1 and G2/M in DNA profiles, and percentage of MPM-2 and pS10 Histone H3 positive cells.

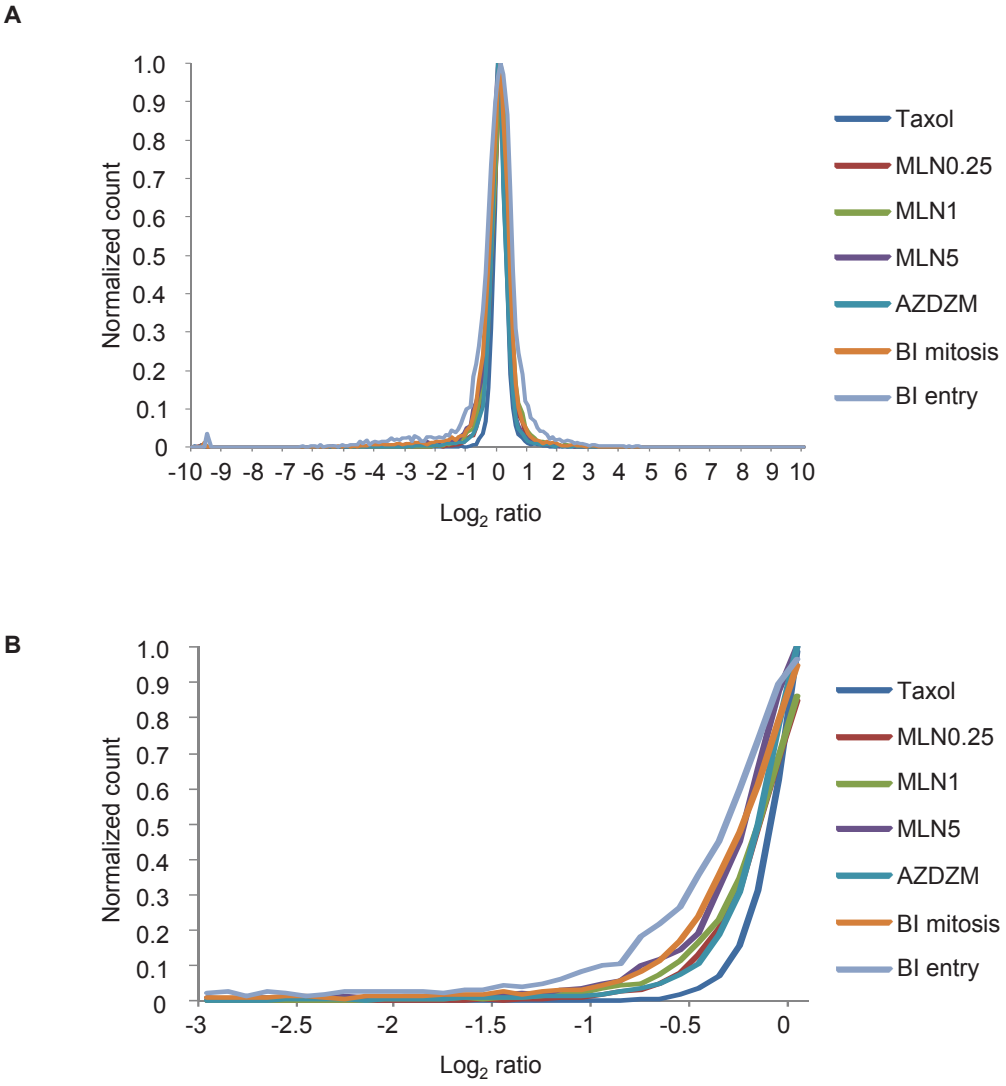

Fig. S5. Ratio distributions. (**A**) Heavy/light ratios of all quantified ModSites were $\log_2$ transformed, normalized and plotted. Heavy Taxol-treated samples were compared to Taxol-treated light samples as the control. AZDZM represents the combined results of the AZD1152- or ZM447439-treated cells. (**B**) Enlargement of the $\log_2$ ratio space between 0 and -3 from panel A.

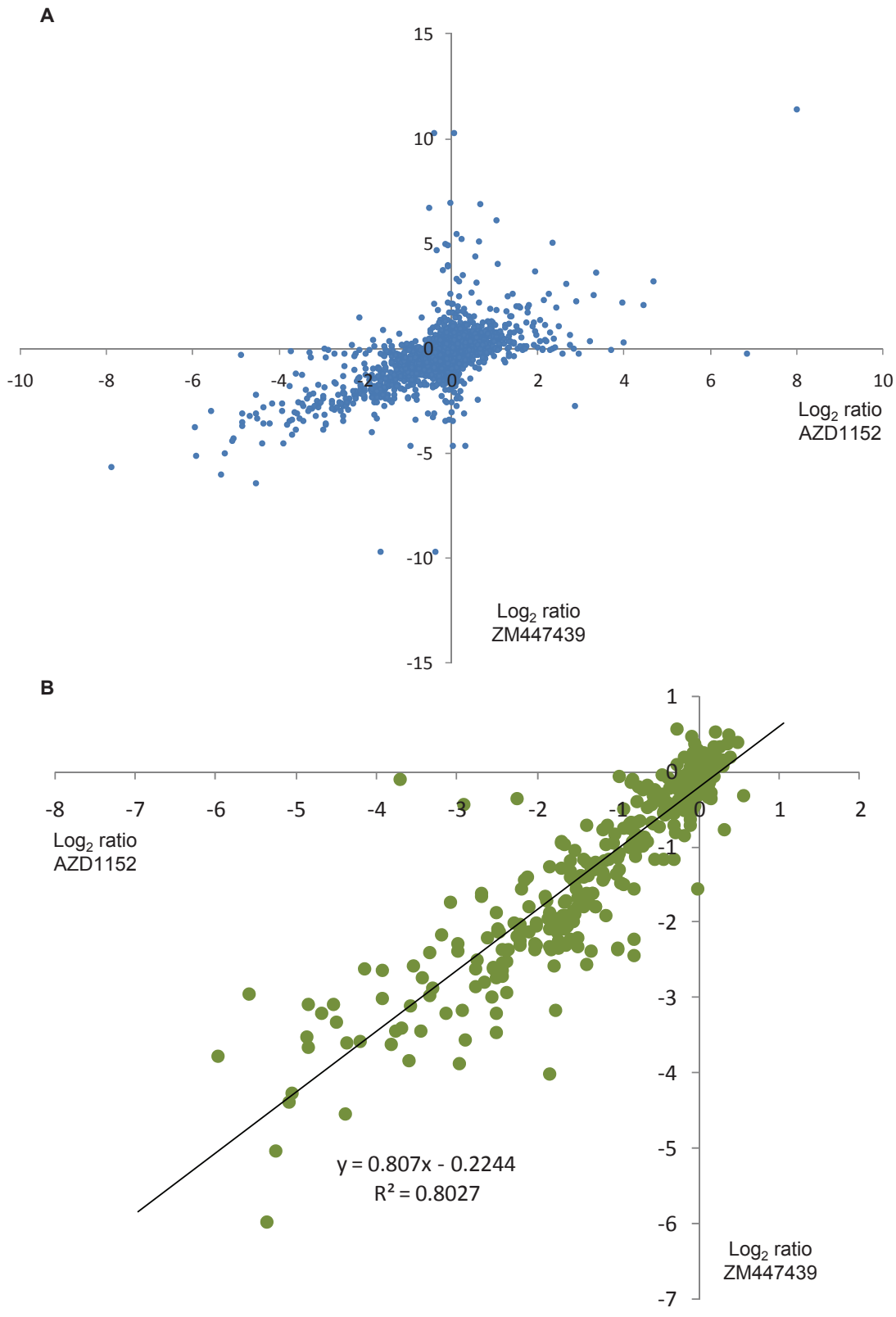

Fig. S6. Comparison of the heavy to light ratios in AZD1152- or ZM447439-treated cells. (**A**) Correlation plot for all 11,206 ModSite ratios that occurred in both of the AZD1152 and ZM447439 datasets. Because most of these ModSites were not AZD1152 or ZM447439 sensitive (random distribution of ModSite ratios similar to Taxol/Taxol control), no significant correlation is anticipated from the bulk of these ModSite ratios. (**B**) Correlation plot for those ModSite ratios that were generated for all candidate Aurora A, Aurora B, and Aurora-ambiguous ModSites listed in table S4 for which values are present in both the AZD1152 and ZM447439 conditions. Note the high degree of correlation between these two biological replicate experiments performed with different Aurora B inhibitors.

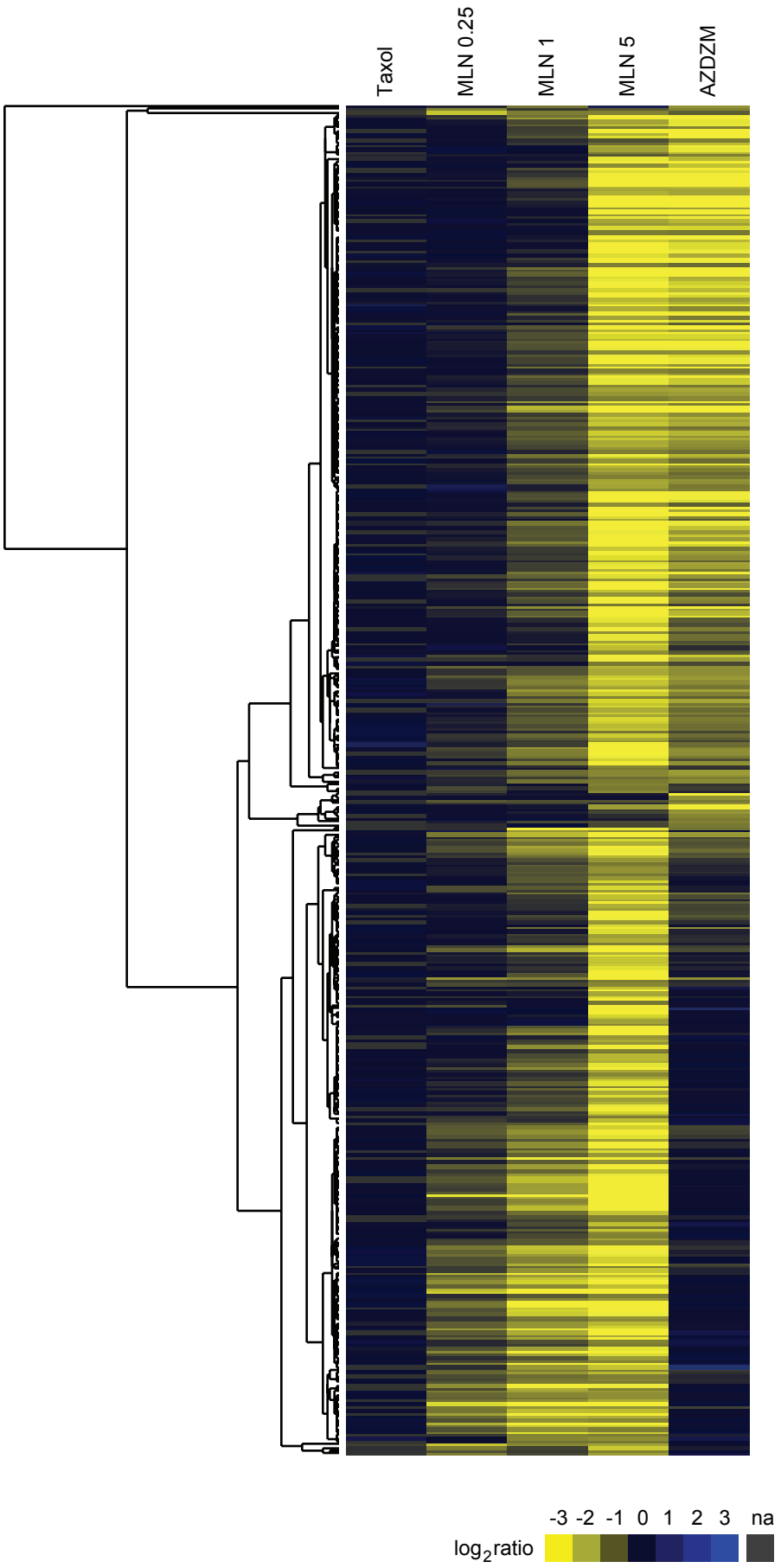

Fig. S7. Candidate Aurora A versus B targets. Hierarchical clustering output for the ModSite array used to distinguish Aurora A from Aurora B candidate substrates. AZDZM represents the combined results of the AZD1152- or ZM447439-treated cells.

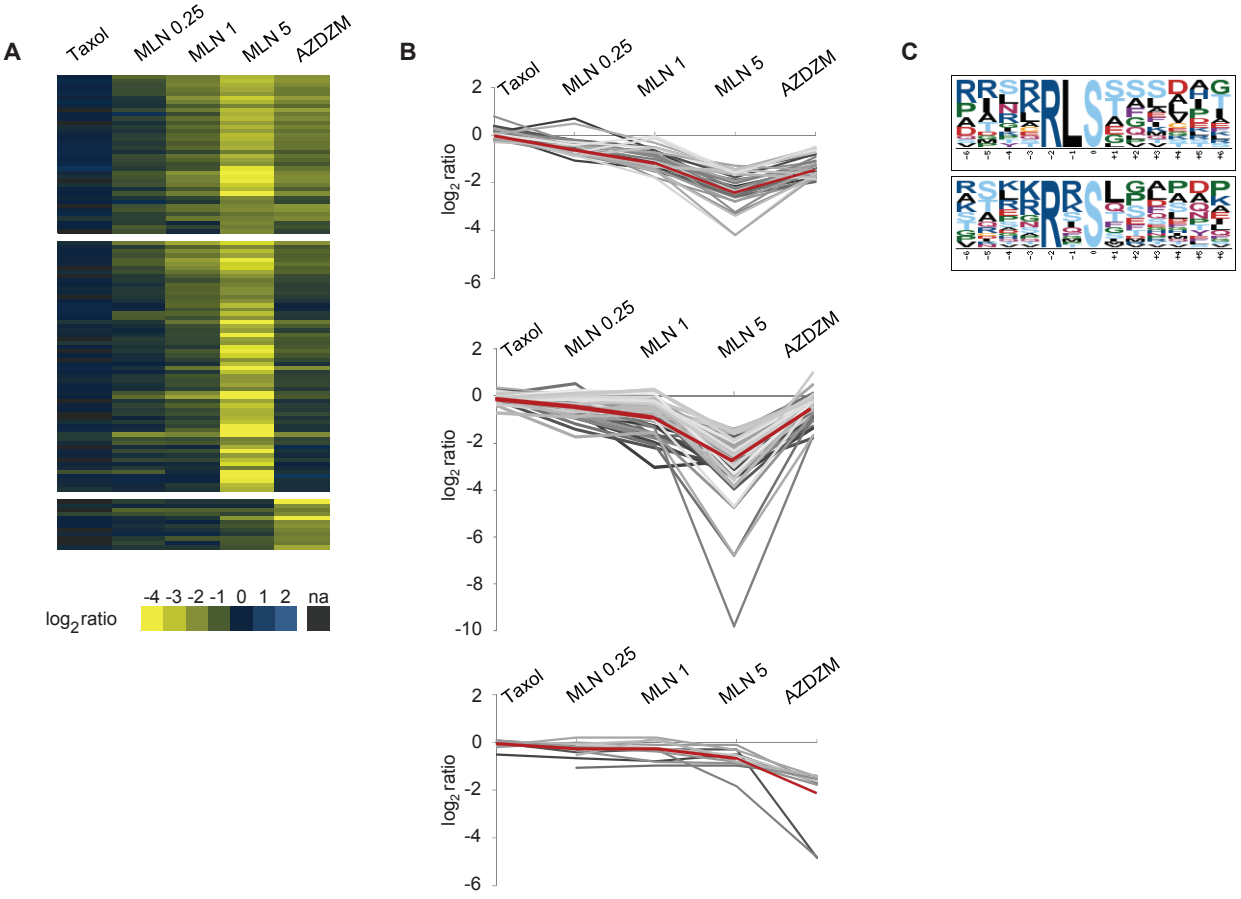

Fig. S8. Cluster and motif analysis of ambiguous Aurora substrates. (**A**) Ambiguous subclusters of Aurora substrates that remain after Aurora A- and Aurora B-specific subclusters have been identified. (**B**) Line graphs of $\log_2$ ratios of the ModSites of the three ambiguous Aurora subclusters from panel A. The red line represents the average. (**C**) Motif analysis of all ambiguous Aurora phosphorylation sites.

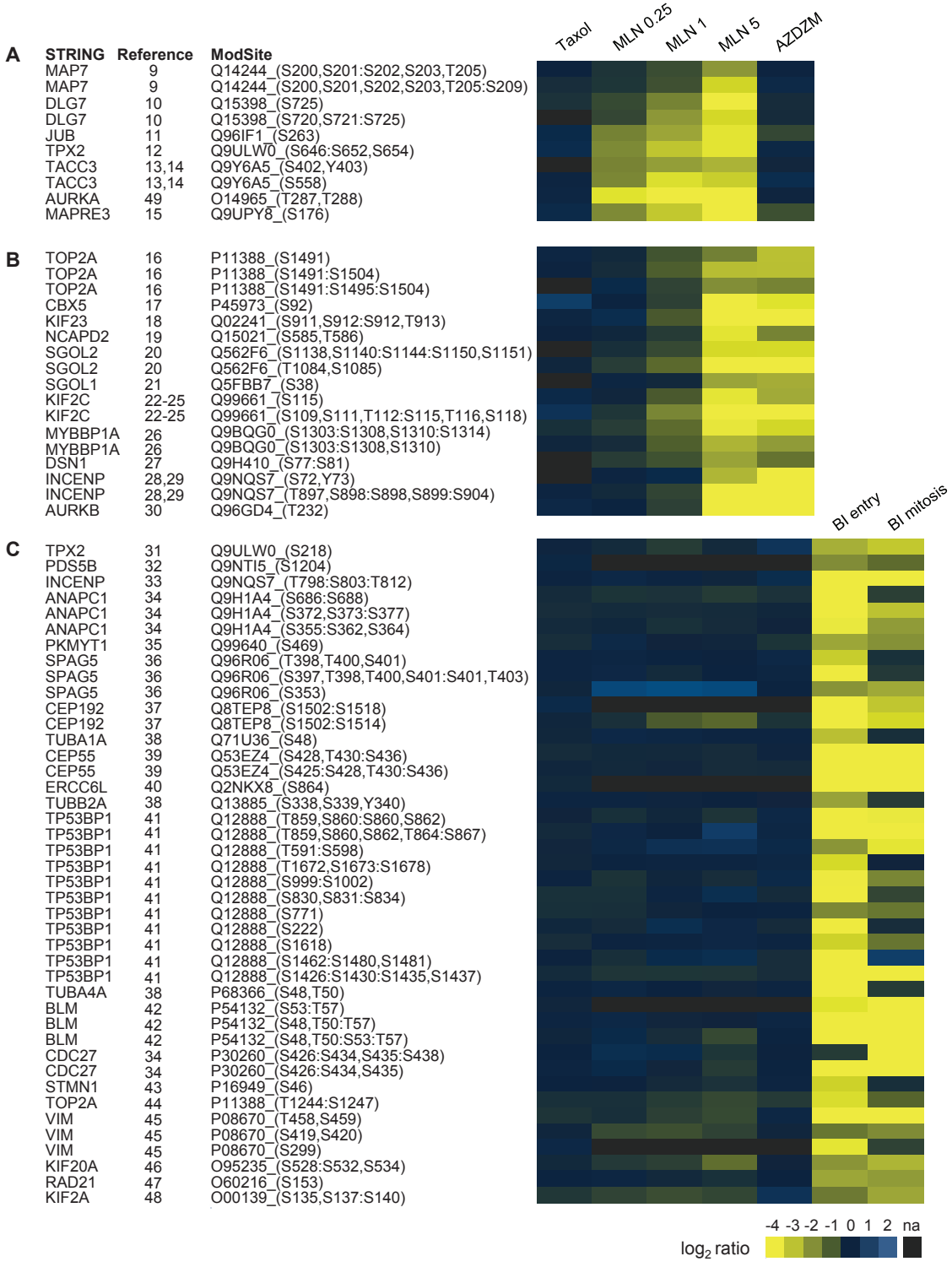

Fig. S9. Log_2 ratio distribution of known Aurora A, Aurora B, and Plk1 substrates identified in this analysis. (**A**) Known Aurora A substrates. (**B**) Known Aurora B substrates. (**C**) Known Plk1 substrates.

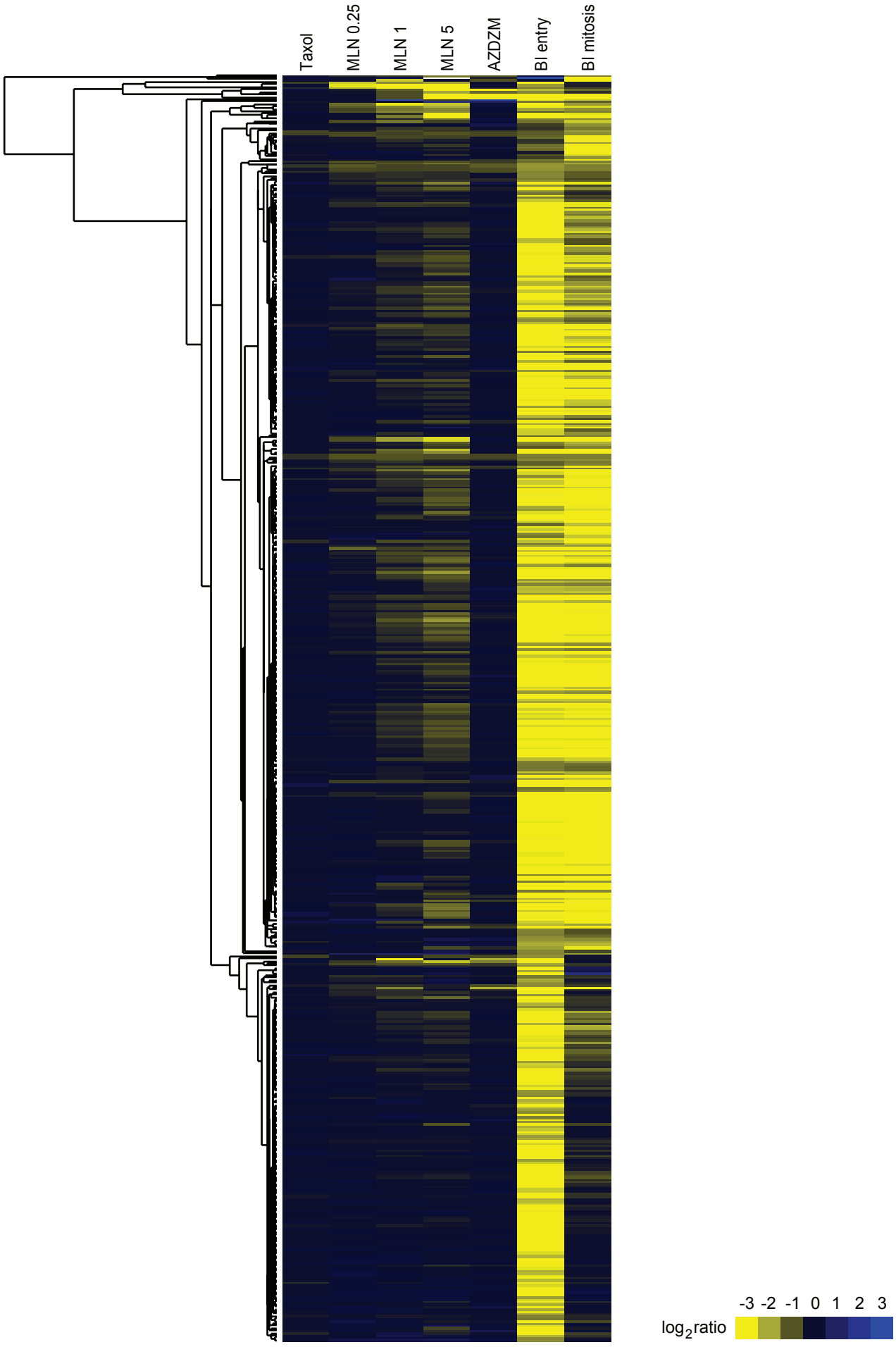

Fig. S10. Candidate Plk targets. Hierarchical clustering output for the ModSite array used to classify Plk candidate substrates.

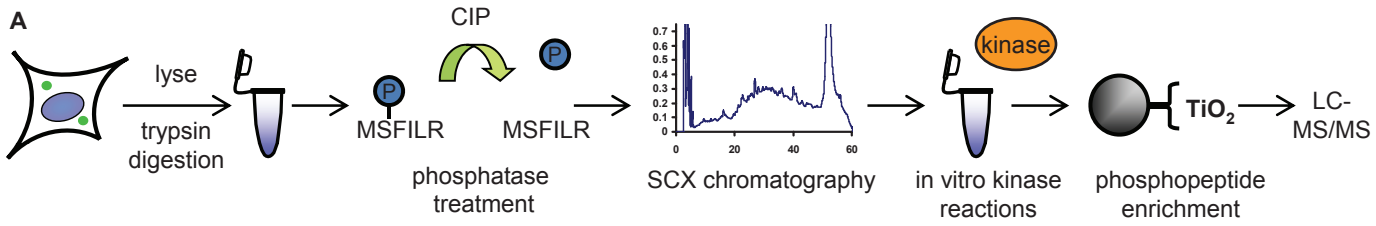

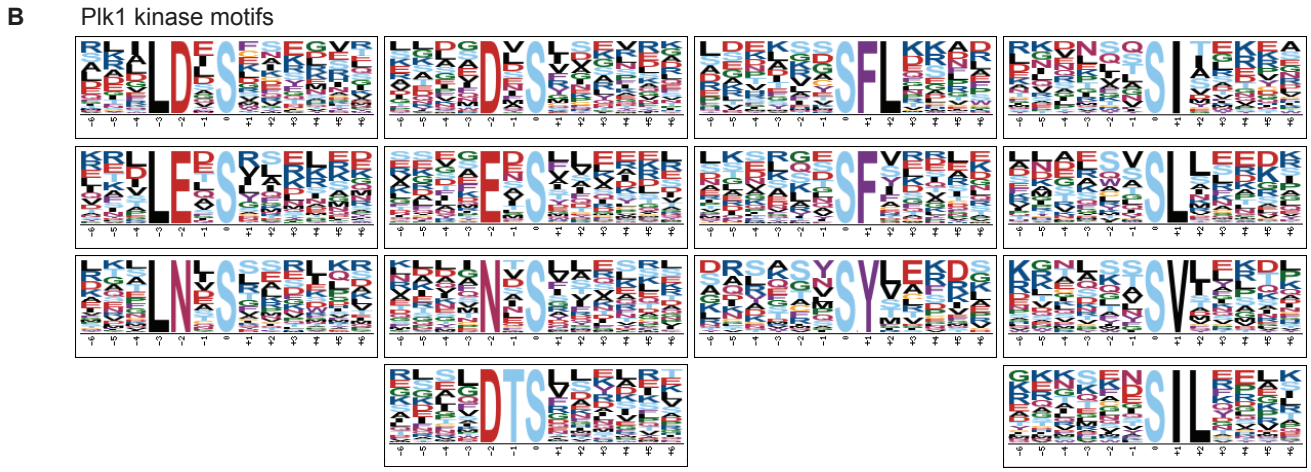

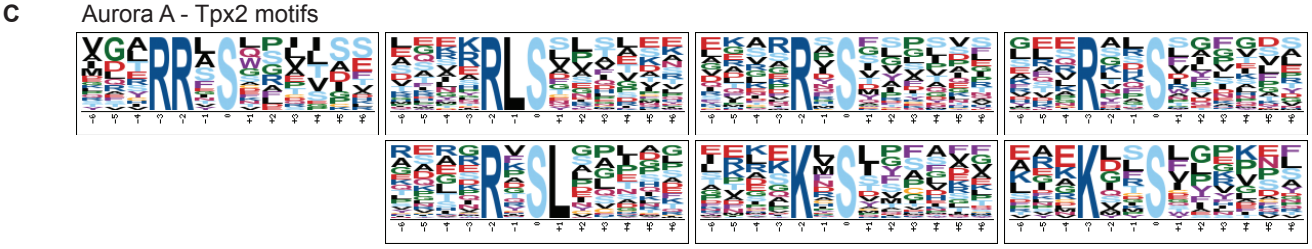

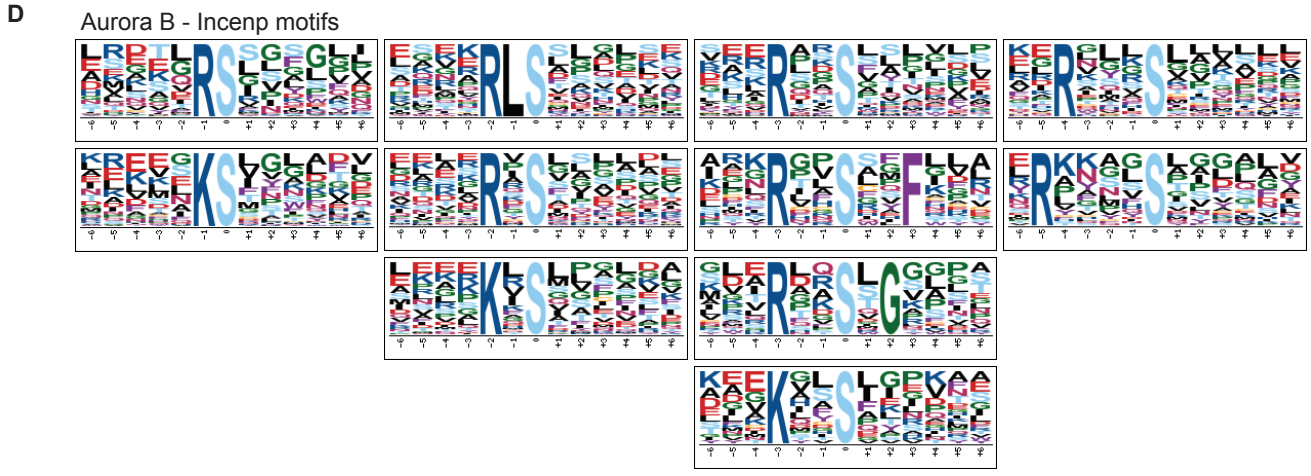

Fig. S11.: In vitro peptide kinase motif assay. (**A**) Scheme of strategy to identify kinase-specific phosphorylation motifs using purified kinase and peptide substrate pools. Asynchronous HeLa cells were lysed and digested with trypsin, and digested lysates were exhaustively dephosphorylated with calf intestinal phosphatase (CIP) and lambda phosphatase. Peptides were separated by SCX chromatography into fractions, phosphorylated in vitro using purified kinase, treated with titanium dioxide microspheres to isolate the resultant phosphopeptides, and analyzed by LC-MS/MS. (**B**) Motif analysis of Plk1 phosphorylation sites identified in the in vitro phosphorylation assay. (**C**) Motif analysis of Aurora kinase A – TPX2 phosphorylation sites identified in the in vitro phosphorylation assay. (**D**) Motif analysis of Aurora kinase B – Incenp phosphorylation sites identified in the in vitro phosphorylation assay.

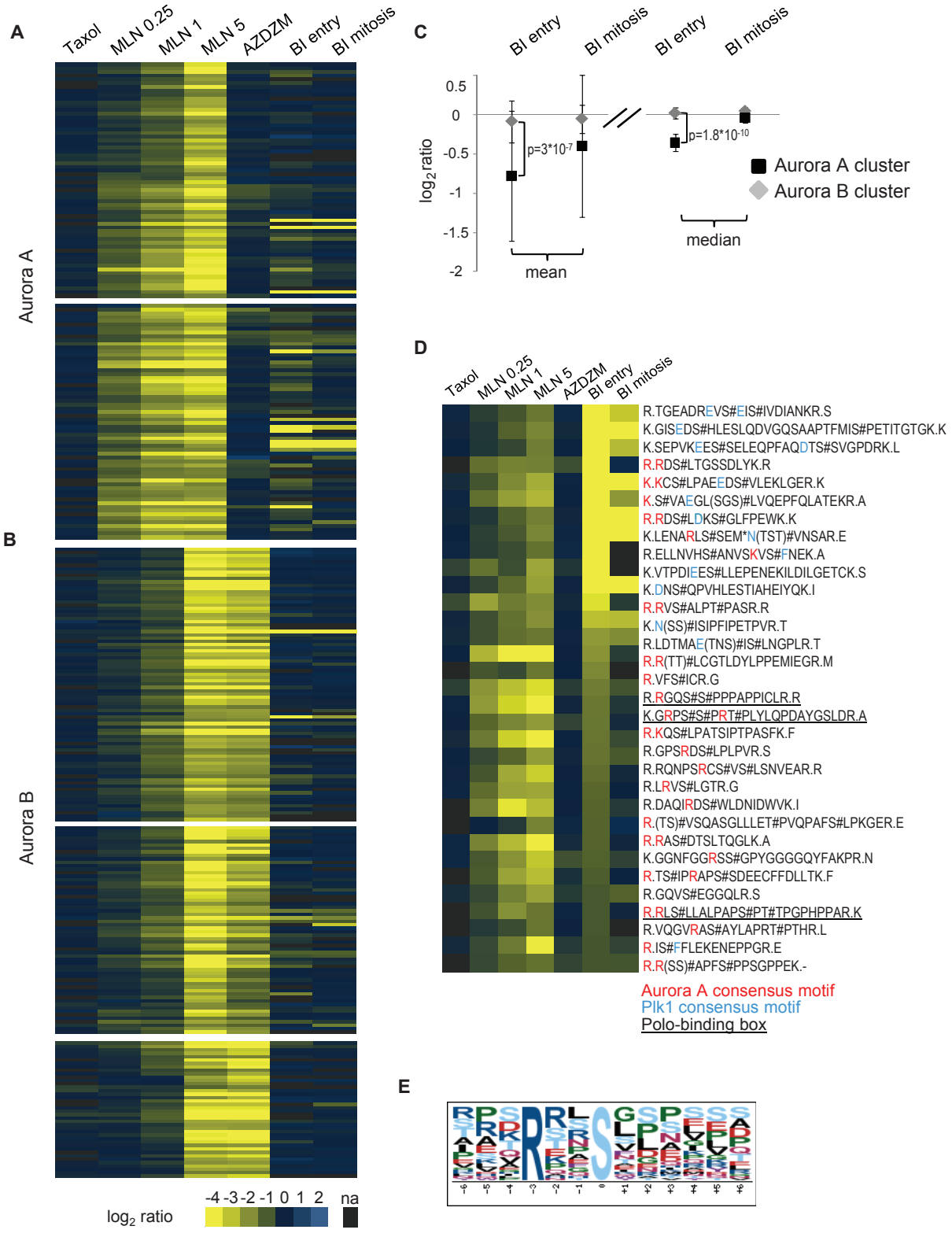

Fig. S12. Regulation of Aurora A by Plk. (**A**) Aurora A subclusters with values for BI entry and BI mitosis conditions added for each ModSite. (**B**) Aurora B subclusters with values for BI entry and BI mitosis conditions added for each ModSite. (**C**) Averaged ratio for ModSites in the Aurora A cluster and Aurora B cluster, as well as ModSites with $\log_2$ ratios less than -1.4 in either BI entry or BI mitosis. Error bars indicate one standard deviation, and p-values indicate statistical significance (Welch's t-test). (**D**) ModSites from the Aurora A cluster with log2 inhibitor/control ratio values in BI entry of less than -0.8. Residues consistent with an Aurora A motif are indicated in red, Plk1 motif in blue, and peptides containing a phosphorylated Polo-binding box (PBD) are underlined. (**E**) Motif analysis of ModSites in the -0.4 BI entry $\log_2$ ratio space yields a motif consistent with Aurora kinases.

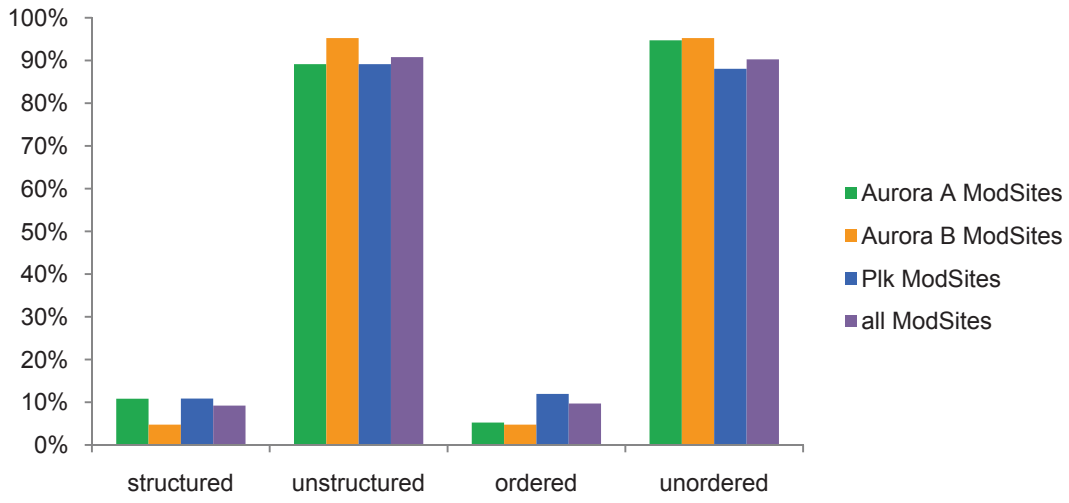

Fig. S13. Prediction of phosphorylation sites in structured and ordered regions of proteins. The bar diagram depicts the percentage of candidate Aurora A, Aurora B, Plk, and all ModSites combined in structured or unstructured, as well as ordered or unordered, protein regions.

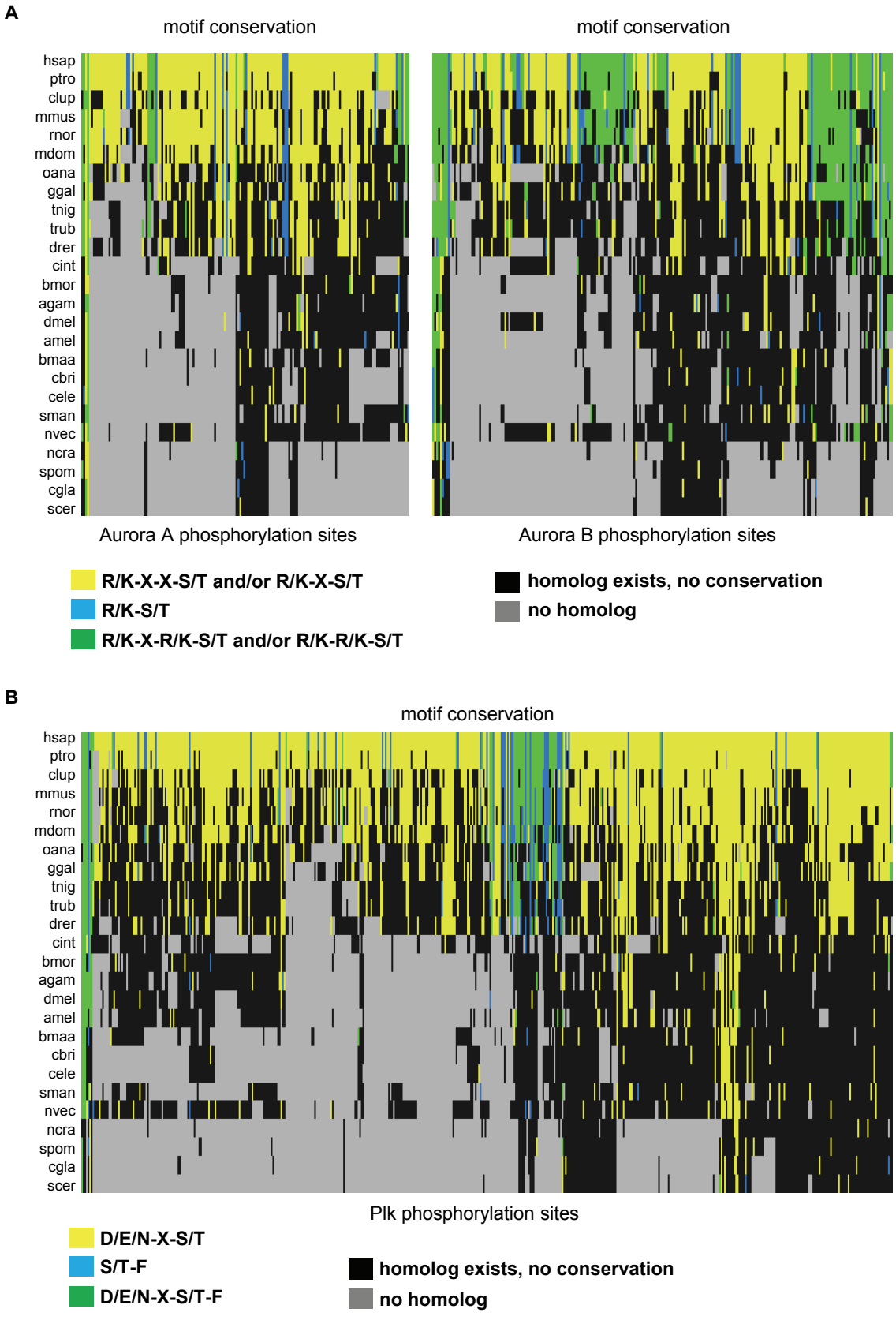

Fig. S14: Evolutionary motif conservation. Hierarchical clustering of evolutionary motif conservation of candidate Aurora A, Aurora B (**A**), and Plk (**B**) ModSites. Rows represent different species, columns represent different ModSites.

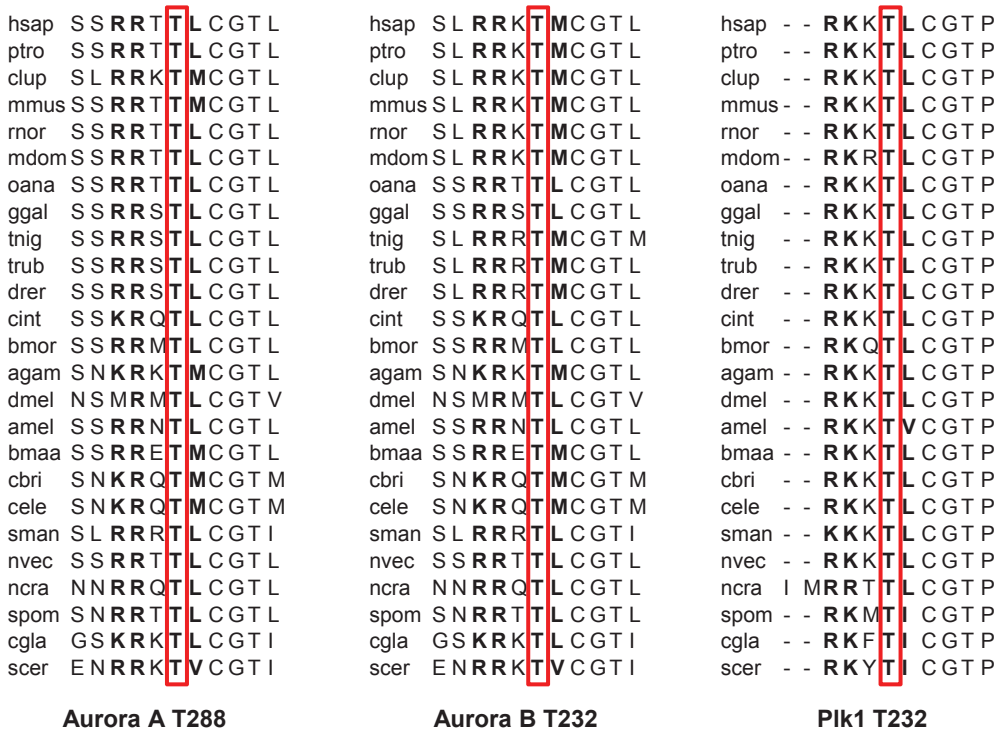

Fig. S15. T-loop sequence alignments. Sequence alignments of Aurora A, Aurora B, and Plk1 from 25 species shows that not only are the kinase-activating phosphorylation sites (Aurora A T288, Aurora B T232, and Plk1 T210) highly conserved, but the surrounding motif elements in the -2, -1, and +1 positions are also conserved.

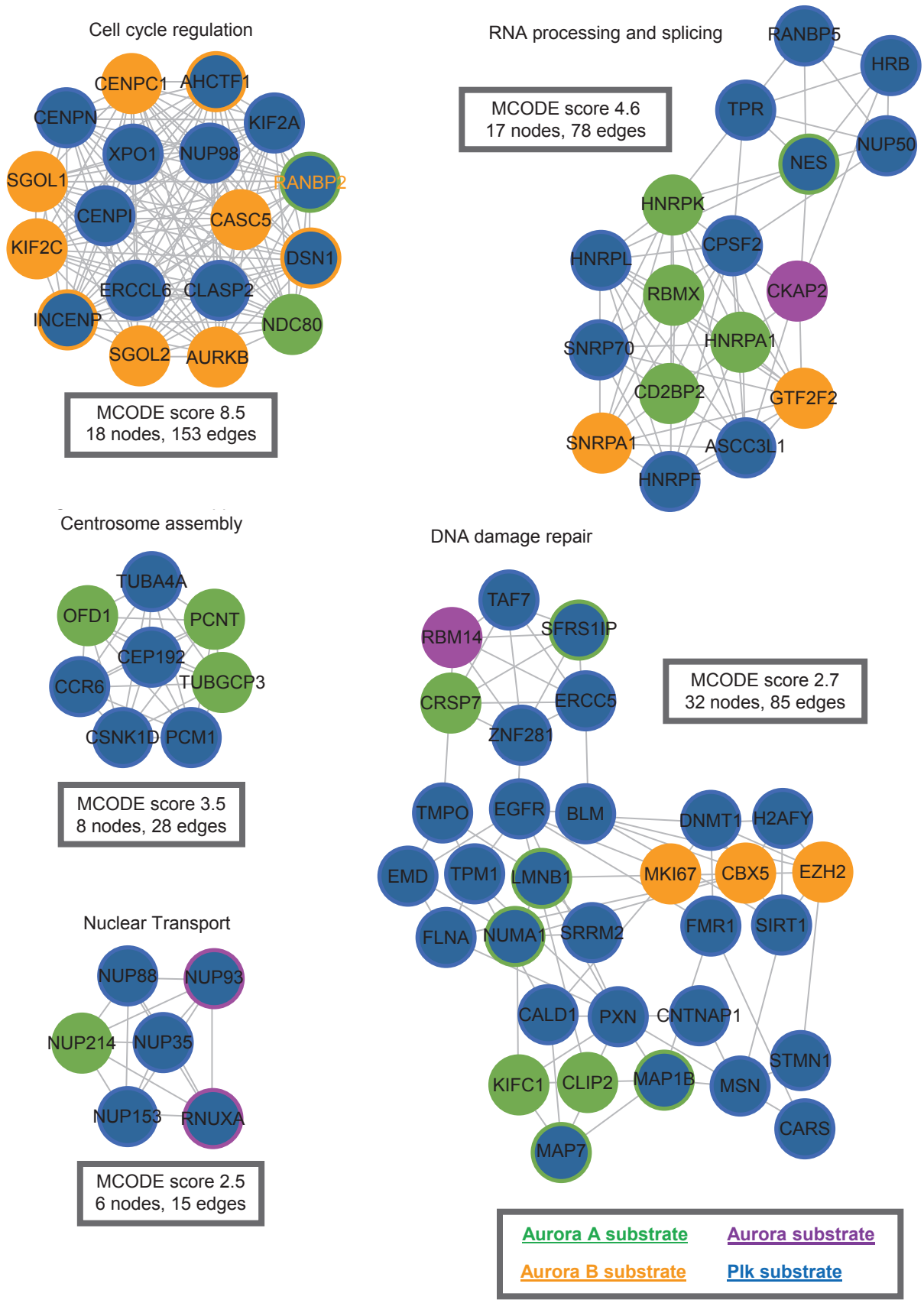

Fig. S16. STRING and MCODE analysis of proteins predicted to be phosphorylated by Aurora A, Aurora B, or Plk. Protein-protein interaction networks of substrate proteins from all three kinases was determined by STRING. Depiction of the top five-ranked clusters from this analysis as determined by MCODE. MCODE score and number of nodes and edges are indicated. Aurora A substrates are indicated in green, Aurora B substrates in orange, ambiguous Aurora substrates in purple, and Plk substrates in blue. Proteins with multiple colors are phosphorylated by more than one kinase. For example, RANBP2 has phosphorylation sites recognized by Aurora A, Aurora B, and Plk.

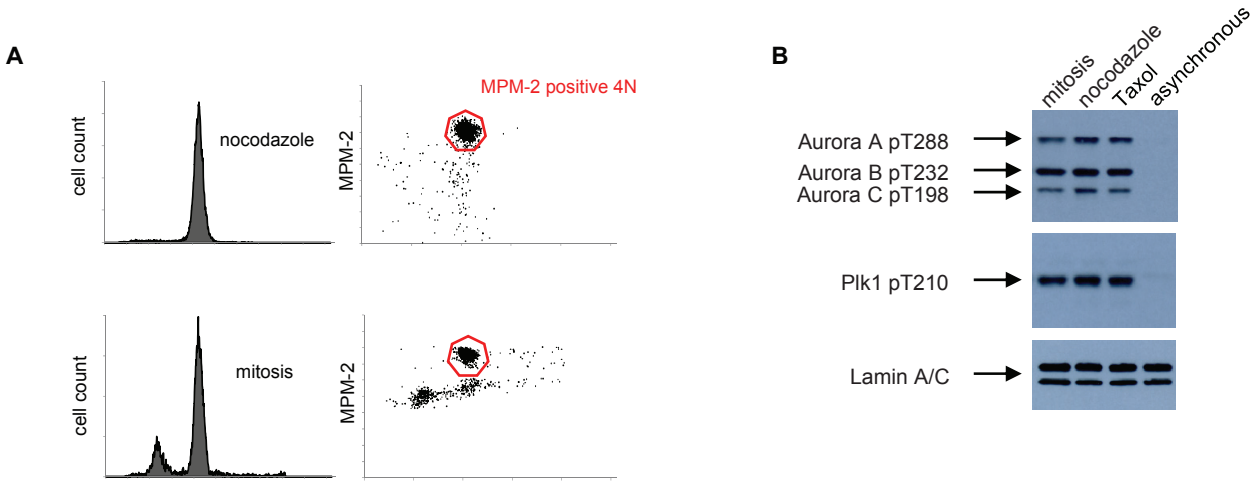

	mitosis	nocodazole
G1	16.7%	3.2%
G2/M	76.7%	93.9%
MPM-2	64.4%	88.3%
pS10 H3	64.1%	87.4%

Fig. S17. Western blot and flow cytometry analysis of nocodazole-arrested HeLa cells and HeLa cells collected by mitotic shake-off after thymidine release. (**A**) Flow cytometry profiles of DNA content and MPM-2 staining of nocodazole-arrested HeLa cells and HeLa cells collected by mitotic shake-off after release from double thymidine block. Table indicates the percentage of cells in G1 and G2/M in DNA profiles, as well as percentage of cells positive for MPM-2 or pS10 Histone H3. (**B**) Western blot of mitotic HeLa cells collected by mitotic shake-off after release from thymidine arrest, HeLa cells arrested in mitosis by nocodazole or Taxol, and asynchronous HeLa cells. Proteins were detected with antibodies recognizing the indicated phosphorylated mitotic kinase or lamin A/C as a loading control

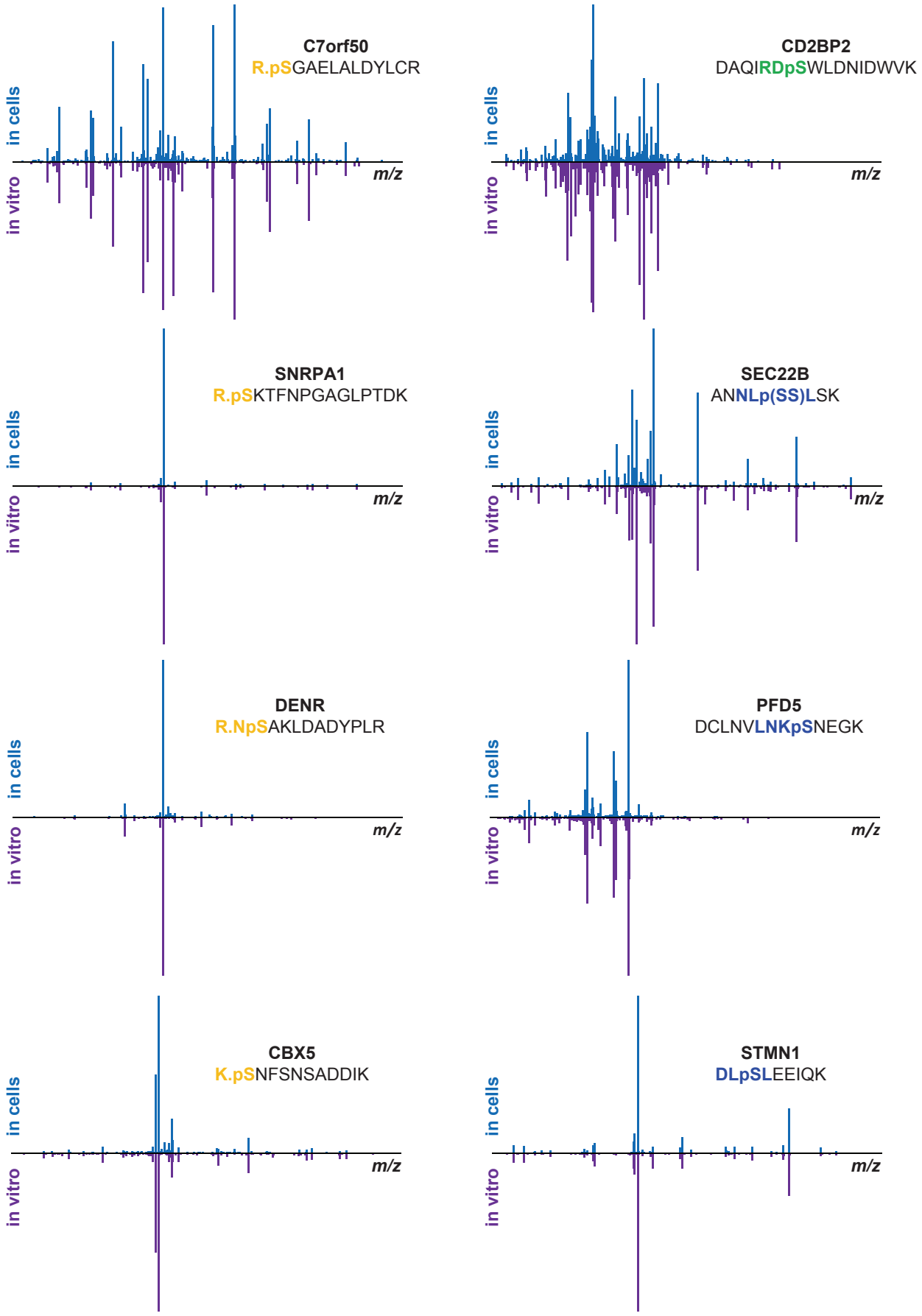

Fig. S18. Reciprocal plots of mass spectrometry results from in vitro kinase reactions and cellular proteomics analysis. Reciprocal plots of MS2peptide fragmentation spectra identified in cells as part of the large-scale proteomics analysis and in vitro kinase reactions for the Aurora B substrates C7orf50, SNRPA1, DENR, and CBX5; Aurora A substrate CD2BP1; and the Plk substrates Sec22B, PFD5, and STMN1.

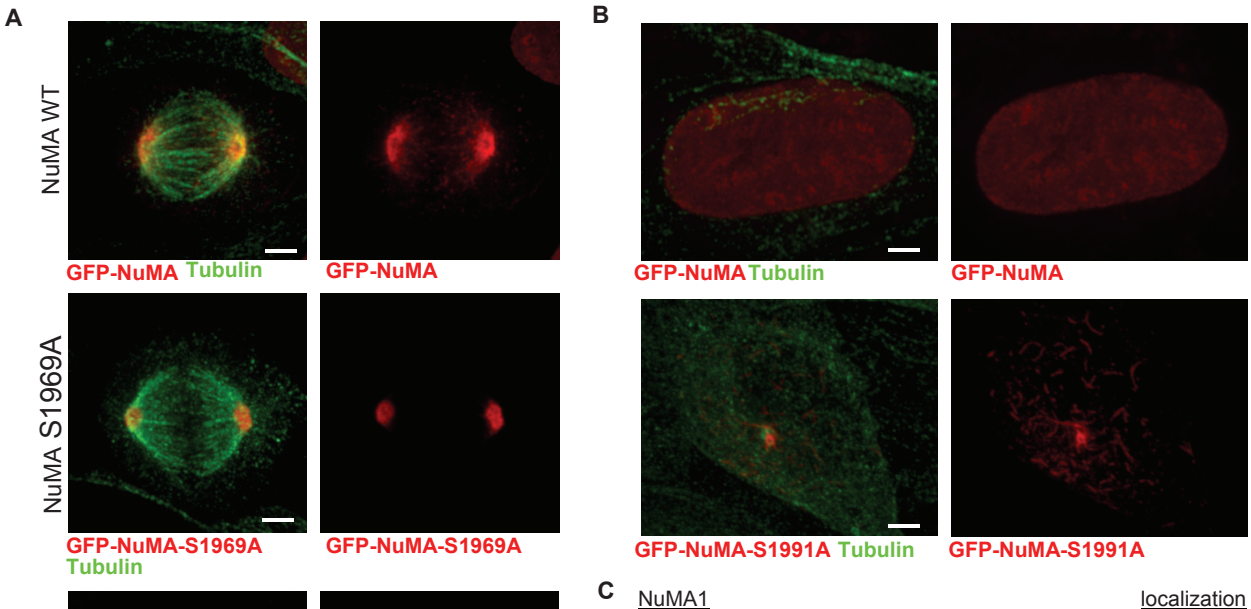

C

NuMA1	localization
WT	spindle
S1788A/S1789A	spindle
S1818A/S1820A	spindle
S1833A/S1834A	spindle
S1788A/S1789A/S1833A/S1834A	spindle
S1788A/S1789A/S1818A/S1820A/S1833A/S1834A	spindle
S1811A/S1812A	spindle
S1811A/S1812A/S1862A/S1868A	spindle
S1862A/S1868A	spindle
S1969A	pole
S1969E	spindle
S1991A	NLS
S2047A	spindle

Fig. S19. The effect NuMA phosphorylation on NuMA localization. (**A**) Micrographs of the indicated green fluorescent protein (GFP)-NuMA fusion protein (red) and microtubules stained with an antibody that recognizes tubulin (green) in HeLa cells in metaphase. (B) Fluorescence images of the indicated GFP-NuMA fusion protein (red) and tubulin (green) in metaphase cells. In panels A and B, the images are maximum z-projections of selected spinning disc confocal optical sections. Scale bar is 3 μm. (C) Table summarizing NuMA mutants and their phenotypes. NLS, nuclear localization sequence Pole, spindle pole and pericentriolar region. At least one hundred cells were scored.

Details Regarding Data Availability

Raw mass spectrometry data files have been submitted to Tranche. Hash codes are as follows:

1) Taxol:

yZvu2oEGflJA+aypAEwlCqPOzde5znxjO8U3ELwiKwVBolndbzYPTaVLRIQjcgAvb32Hajgv/S+mRz
DJsgpPUzNxM3QAAAAAAAAWWA==

2) MLN0.25 (1 of 4):

NVtqbw3KbeXvlBRTaqBvCz8fH1cQd9RhRq6XQ1b1g5wOZzgFFLKgRG4hFZsNoU8a57zCqf+A6bs
WXWUDOwKxSMAmGjgAAAAAAAANnQ==

3) MLN0.25 (2 of 4):

EXd9hXsD+KHKGi36ehCeLpdR1kExgyaDSwivRIVAhNtx98xrO1dQL5hAUMWSX5AVgEUITb7aw
a7xRTOR/a4fTJ6WcNkAAAAAAAAJRg==

4) MLN0.25 (3 of 4):

Poo2J7gvOt6fYgbE2Z1P+mGj95HunFJHv0WJkww5woi2Aw3OHH9oYM8ZyYR8s05+uvK6MDM0u
ysKzvym7Is1jAO6YgsAAAAAAAAS3g==

5) MLN0.25 (4 of 4):

dIUHZNAh3K7aebXsMDptMkoVprktbQ+ZwgBWFbvNP2eP+guoFl0oYXFBmueH739CjZBKXccLZ
GorgoqSXFNKd02Q/AIAAAAAAAAK9Q==

6) MLN1 (1 of 4):

CXEY1ikEM7az7IVXAs/SJjcK6OV9pnDrBxXw32TeLPPyDv1+Y+a7l+0asSIsjOSzy40V6H2E2vDr6P
+zkt3q0+5/ExMAAAAAAAANtg==

7) MLN1 (2 of 4):

Yqg2Reqe/zhenOz+CV3mfiOoNjezqJdo3qba5fOuXilpQGm9m1VrcGRkXvL739ZO9J7zCDc6yQ7Yz
VckBJaulBvlG5EAAAAAAAAOsA==

8) MLN1 (3 of 4):

2iSaEurZSibWcydKzazfCCGnxCSEsmwzPyBywQO29DfoyM7ouHiIeEUwO6II31bJWtznG0zMFQcW
nS3YvQE91HUWC/oAAAAAAAAQ8w==

9) MLN1 (4 of 4):

ISe4MrpjbxXqH4LFNXAOiCi8RWpIFMtKjhzgMQNtKJVgpE45oxbmiKXMZVfPfpovDZNBDIGDG
qYhelgQkkSBuXMKEcEAAAAAAAAOrw==

10) MLN5 (1 of 2):

z14avfdbuqQD7HBcn4MSK+05H2BAEjYYTbIxzi7G0ZEGfkuoH5PamUgFfSA/5C4fJfGtdfk0eo/sl/Dx
eflhssg2cTgAAAAAAAALyQ==

11) MLN5 (2 of 2):

6oT77guljsJwL2olcPYwgpMVBk7/pgrqgzvWqYLmrQnGWpexz2Mjm2dMxbnbKGyWVImVUBg4kw
A9i0JZ9qQ4XmTg2ZYAAAAAAAAM7A==

12) AZDZM (1 of 4):

gnGZtCfwTK/JHQzfKXIJxURJH9wV+sjW/79FGppYTDI7QSFWDIka8DYMlMbjypr/nSZ7/cCV5GA
IhMiX3YbkXrUMuuUAAAAAAAAP3Q==

13) AZDZM (2 of 4):

6C0x7Z1sFszLvlq/3ka6xNxYrkbZreRunRXo2gPbg8FBmetHbZDNxObw2lquCvCIre8016JDHPXf/9o
MbEAjUo2aA3MAAAAAAAAQlg==

14) AZDZM (3 of 4):

bGonsM+aKXN9rCIojSO5ONmQnBLCdWgnwmLvjpVa3PZniKTHi9AJwAiNu7ZwVwHcsCRd06ad6
3NWSg6K+sqAozEeXZ0AAAAAAAANNg==

15) AZDZM (4 of 4):

e7FiityhPJHj55v1U/F2xg8+rqGMmyCIPGRMTdpz2fdDsGMyTCg90lOuNDiXJxNRmDMgRjVe4cY4

YiJUzz/DLx5NT5EAAAAAAAARbA==

16) BI entry:

DYmrNkDRx1WVGe76DuZVWhaxVw6H2x6+Ku9+aem2t+7EyD60OrywqFDVYMEKUKF6DsuV0

O7S033zE0tJZv9FFE+ztG8AAAAAAAAXAw==

17) BI mitosis:

mopDwxnvEwWkYbVqrYvOCXKFGCCy702E5nCownwHf7JjHhwhA6/g9+RFB8KxYzyXtI+5hsxPY

WZorkNv0XSoQ4DsCUYAAAAAAAWfA==

Description of tables S1-S6

Table S1. Complete list of all ModSites and representative peptides. UniProt ACC, UniProt accession; UniProt Name, UniProt protein identifier; XCorr, SEQUEST cross-correlation score; dCn, SEQUEST delta-correlation score; MMA (PPM), mass measurement accuracy in parts per million; Olsen, 2010 (*7*); Dephoure, 2008 (*8*).

Table S2. ModSites assigned to the Aurora kinase substrate cluster. Cluster 3.0 output file containing ModSites, gene names, protein descrioptions, and corresponding $\log_2$ ratios across all relevant treatment conditions. Gene names and protein descriptions are defined from UniProt. Tax, Taxol-arrested cells; MLN250, MLN8054 250 nM; MLN1, MLN8054 1 μM; MLN5, MLN8054 5 μM; AZDZM, combined results from both the AZD1152 (1 μM concentration) and ZM447439 (5 μM concentration).

Table S3. ModSites assigned to the Plk substrate cluster. Cluster 3.0 output file containing ModSites, gene names, protein descrioptions, and corresponding $\log_2$ ratios across all relevant treatment conditions. Tax, Taxol-arrested cells; MLN250, MLN8054 250 nM; MLN1, MLN8054 1 μM; MLN5, MLN8054 5 μM; AZDZM, combined results from both the AZD1152 (1 μM concentration) and ZM447439 (5 μM concentration); BI entry, 0.1 μM BI2536-treated HeLa cells entering mitosis; BI mitosis, 0.1 μM BI2536-treated HeLa cells arrested at metaphase with Taxol.

Table S4. Analysis of site- and motif-conservation for candidate Aurora A, B, and Plk substrates across evolution. Rows represent species (see Supplementary Materials Methods for details), columns represent ModSites. Last two rows provide protein accessions and protein descriptions. 5 (green) [R/K]X[R/K][S/T] and/or [R/K][R/K][S/T]; 4 (blue) [R/K][S/T]; 3 (yellow) [D/E/N]X[S/T]; 0 (gray) no

homolog; black homolog exists, no conservation. Aurka_sites and Aurka_motif, ModSites and motifs in the Aurora A cluster; Aurkb_sites and Aurkb_motif, ModSites and motifs in the Aurora B cluster; plk_sites and plk_motifs, ModSites and motifs in the Plk cluster.

Table S5. ModSite assignments to Aurora A, Aurora B, Aurora ambiguous, and Plk clusters. Heavy/light log2 ratios from the indicated conditions (see tables S1 and S2 for definitions). Async, asynchronous cells; Olsen, 2010 (*7*); Dephoure, 2008 (*8*).

Table S6. Plk1-interacting proteins. Proteins identified in duplicate Plk1 immunoprecipitation experiments by total peptide count. Proteins identified in duplicate unspecific IgG control immunoprecipitation experiments by peptide count. Only those proteins identified by 6-fold more total peptides across the union of the two experiments versus the union of the two control IgG experiments are considered Plk1 interactors.

SUPPLEMENTARY REFERENCES

1. F. Chen, A. J. Mackey, C. J. Stoeckert, Jr., D. S. Roos, OrthoMCL-DB: querying a comprehensive multi-species collection of ortholog groups. *Nucleic Acids Res* **34**, D363-368 (2006).
2. R. C. Edgar, MUSCLE: a multiple sequence alignment method with reduced time and space complexity. *BMC Bioinformatics* **5**, 113 (2004).
3. D. T. Jones, Protein secondary structure prediction based on position-specific scoring matrices. *J Mol Biol* **292**, 195-202 (1999).
4. J. J. Ward, J. S. Sodhi, L. J. McGuffin, B. F. Buxton, D. T. Jones, Prediction and functional analysis of native disorder in proteins from the three kingdoms of life. *J Mol Biol* **337**, 635-645 (2004).
5. L. J. Jensen, M. Kuhn, M. Stark, S. Chaffron, C. Creevey, J. Muller, T. Doerks, P. Julien, A. Roth, M. Simonovic, P. Bork, C. von Mering, STRING 8--a global view on proteins and their functional interactions in 630 organisms. *Nucleic Acids Res* **37**, D412-416 (2009).
6. P. Shannon, A. Markiel, O. Ozier, N. S. Baliga, J. T. Wang, D. Ramage, N. Amin, B. Schwikowski, T. Ideker, Cytoscape: a software environment for integrated models of biomolecular interaction networks. *Genome Res* **13**, 2498-2504 (2003).
7. J. V. Olsen, M. Vermeulen, A. Santamaria, C. Kumar, M. L. Miller, L. J. Jensen, F. Gnad, J. Cox, T. S. Jensen, E. A. Nigg, S. Brunak, M. Mann, Quantitative phosphoproteomics reveals widespread full phosphorylation site occupancy during mitosis. *Sci Signal* **3**, ra3 (2010).
8. N. Dephoure, C. Zhou, J. Villen, S. A. Beausoleil, C. E. Bakalarski, S. J. Elledge, S. P. Gygi, A quantitative atlas of mitotic phosphorylation. *Proc Natl Acad Sci U S A* **105**, 10762-10767 (2008).
9. T. Sardon, R. A. Pache, A. Stein, H. Molina, I. Vernos, P. Aloy, Uncovering new substrates for Aurora A kinase. *EMBO Rep* **11**, 977-984 (2010).
10. C. T. Yu, J. M. Hsu, Y. C. Lee, A. P. Tsou, C. K. Chou, C. Y. Huang, Phosphorylation and stabilization of HURP by Aurora-A: implication of HURP as a transforming target of Aurora-A. *Mol Cell Biol* **25**, 5789-5800 (2005).
11. T. Hirota, N. Kunitoku, T. Sasayama, T. Marumoto, D. Zhang, M. Nitta, K. Hatakeyama, H. Saya, Aurora-A and an interacting activator, the LIM protein Ajuba, are required for mitotic commitment in human cells. *Cell* **114**, 585-598 (2003).
12. T. A. Kufer, H. H. Sillje, R. Korner, O. J. Gruss, P. Meraldi, E. A. Nigg, Human TPX2 is required for targeting Aurora-A kinase to the spindle. *J Cell Biol* **158**, 617-623 (2002).
13. P. J. LeRoy, J. J. Hunter, K. M. Hoar, K. E. Burke, V. Shinde, J. Ruan, D. Bowman, K. Galvin, J. A. Ecsedy, Localization of human TACC3 to mitotic spindles is mediated by phosphorylation on Ser558 by Aurora A: a novel pharmacodynamic method for measuring Aurora A activity. *Cancer Res* **67**, 5362-5370 (2007).
14. K. Kinoshita, T. L. Noetzel, L. Pelletier, K. Mechtler, D. N. Drechsel, A. Schwager, M. Lee, J. W. Raff, A. A. Hyman, Aurora A phosphorylation of TACC3/maskin is required for centrosome-dependent microtubule assembly in mitosis. *J Cell Biol* **170**, 1047-1055 (2005).
15. R. Ban, H. Matsuzaki, T. Akashi, G. Sakashita, H. Taniguchi, S. Y. Park, H. Tanaka, K. Furukawa, T. Urano, Mitotic regulation of the stability of microtubule plus-end tracking protein EB3 by ubiquitin ligase SIAH-1 and Aurora mitotic kinases. *J Biol Chem* **284**, 28367-28381 (2009).
16. C. Morrison, A. J. Henzing, O. N. Jensen, N. Osheroff, H. Dodson, S. E. Kandels-Lewis, R. R. Adams, W. C. Earnshaw, Proteomic analysis of human metaphase chromosomes reveals topoisomerase II alpha as an Aurora B substrate. *Nucleic Acids Res* **30**, 5318-5327 (2002).
17. Y. Terada, Aurora-B/AIM-1 regulates the dynamic behavior of HP1alpha at the G2-M transition. *Mol Biol Cell* **17**, 3232-3241 (2006).
18. R. Neef, U. R. Klein, R. Kopajtich, F. A. Barr, Cooperation between mitotic kinesins controls the late stages of cytokinesis. *Curr Biol* **16**, 301-307 (2006).
19. A. Takemoto, A. Murayama, M. Katano, T. Urano, K. Furukawa, S. Yokoyama, J. Yanagisawa, F. Hanaoka, K. Kimura, Analysis of the role of Aurora B on the chromosomal targeting of condensin I. *Nucleic Acids Res* **35**, 2403-2412 (2007).

20. Y. Tanno, T. S. Kitajima, T. Honda, Y. Ando, K. Ishiguro, Y. Watanabe, Phosphorylation of mammalian Sgo2 by Aurora B recruits PP2A and MCAK to centromeres. *Genes Dev* **24**, 2169-2179 (2010).
21. T. D. Resnick, D. L. Satinover, F. MacIsaac, P. T. Stukenberg, W. C. Earnshaw, T. L. Orr-Weaver, M. Carmena, INCENP and Aurora B promote meiotic sister chromatid cohesion through localization of the Shugoshin MEI-S332 in Drosophila. *Dev Cell* **11**, 57-68 (2006).
22. P. D. Andrews, Y. Ovechkina, N. Morrice, M. Wagenbach, K. Duncan, L. Wordeman, J. R. Swedlow, Aurora B regulates MCAK at the mitotic centromere. *Dev Cell* **6**, 253-268 (2004).
23. R. Ohi, T. Sapra, J. Howard, T. J. Mitchison, Differentiation of cytoplasmic and meiotic spindle assembly MCAK functions by Aurora B-dependent phosphorylation. *Mol Biol Cell* **15**, 2895-2906 (2004).
24. A. L. Knowlton, W. Lan, P. T. Stukenberg, Aurora B is enriched at merotelic attachment sites, where it regulates MCAK. *Curr Biol* **16**, 1705-1710 (2006).
25. X. Zhang, W. Lan, S. C. Ems-McClung, P. T. Stukenberg, C. E. Walczak, Aurora B phosphorylates multiple sites on mitotic centromere-associated kinesin to spatially and temporally regulate its function. *Mol Biol Cell* **18**, 3264-3276 (2007).
26. C. Perrera, R. Colombo, B. Valsasina, P. Carpinelli, S. Troiani, M. Modugno, L. Gianellini, P. Cappella, A. Isacchi, J. Moll, L. Rusconi, Identification of Myb-binding protein 1A (MYBBP1A) as a novel substrate for aurora B kinase. *J Biol Chem* **285**, 11775-11785 (2010).
27. Y. Yang, F. Wu, T. Ward, F. Yan, Q. Wu, Z. Wang, T. McGlothen, W. Peng, T. You, M. Sun, T. Cui, R. Hu, Z. Dou, J. Zhu, W. Xie, Z. Rao, X. Ding, X. Yao, Phosphorylation of HsMis13 by Aurora B kinase is essential for assembly of functional kinetochore. *J Biol Chem* **283**, 26726-26736 (2008).
28. J. D. Bishop, J. M. Schumacher, Phosphorylation of the carboxyl terminus of inner centromere protein (INCENP) by the Aurora B Kinase stimulates Aurora B kinase activity. *J Biol Chem* **277**, 27577-27580 (2002).
29. R. Honda, R. Korner, E. A. Nigg, Exploring the functional interactions between Aurora B, INCENP, and survivin in mitosis. *Mol Biol Cell* **14**, 3325-3341 (2003).
30. Y. Yasui, T. Urano, A. Kawajiri, K. Nagata, M. Tatsuka, H. Saya, K. Furukawa, T. Takahashi, I. Izawa, M. Inagaki, Autophosphorylation of a newly identified site of Aurora-B is indispensable for cytokinesis. *J Biol Chem* **279**, 12997-13003 (2004).
31. F. Eckerdt, G. Pascreau, M. Phistry, A. L. Lewellyn, A. A. DePaoli-Roach, J. L. Maller, Phosphorylation of TPX2 by Plx1 enhances activation of Aurora A. *Cell Cycle* **8**, 2413-2419 (2009).
32. M. L. Baldwin, J. A. Julius, X. Tang, Y. Wang, J. Bachant, The yeast SUMO isopeptidase Smt4/Ulp2 and the polo kinase Cdc5 act in an opposing fashion to regulate sumoylation in mitosis and cohesion at centromeres. *Cell Cycle* **8**, 3406-3419 (2009).
33. H. Goto, T. Kiyono, Y. Tomono, A. Kawajiri, T. Urano, K. Furukawa, E. A. Nigg, M. Inagaki, Complex formation of Plk1 and INCENP required for metaphase-anaphase transition. *Nat Cell Biol* **8**, 180-187 (2006).
34. C. Kraft, F. Herzog, C. Gieffers, K. Mechtler, A. Hagting, J. Pines, J. M. Peters, Mitotic regulation of the human anaphase-promoting complex by phosphorylation. *Embo J* **22**, 6598-6609 (2003).
35. D. Inoue, N. Sagata, The Polo-like kinase Plx1 interacts with and inhibits Myt1 after fertilization of Xenopus eggs. *Embo J* **24**, 1057-1067 (2005).
36. J. Yuan, M. Li, L. Wei, S. Yin, B. Xiong, S. Li, S. L. Lin, H. Schatten, Q. Y. Sun, Astrin regulates meiotic spindle organization, spindle pole tethering and cell cycle progression in mouse oocytes. *Cell Cycle* **8**, 3384-3395 (2009).
37. L. Haren, T. Stearns, J. Luders, Plk1-dependent recruitment of gamma-tubulin complexes to mitotic centrosomes involves multiple PCM components. *PLoS One* **4**, e5976 (2009).
38. Y. Feng, D. R. Hodge, G. Palmieri, D. L. Chase, D. L. Longo, D. K. Ferris, Association of polo-like kinase with alpha-, beta- and gamma-tubulins in a stable complex. *Biochem J* **339 (Pt 2)**, 435-442 (1999).
39. M. Fabbro, B. B. Zhou, M. Takahashi, B. Sarcevic, P. Lal, M. E. Graham, B. G. Gabrielli, P. J. Robinson, E. A. Nigg, Y. Ono, K. K. Khanna, Cdk1/Erk2- and Plk1-dependent phosphorylation of a centrosome protein, Cep55, is required for its recruitment to midbody and cytokinesis. *Dev Cell* **9**, 477-488 (2005).

40. C. Baumann, R. Korner, K. Hofmann, E. A. Nigg, PICH, a centromere-associated SNF2 family ATPase, is regulated by Plk1 and required for the spindle checkpoint. *Cell* **128**, 101-114 (2007).
41. M. A. van Vugt, A. K. Gardino, R. Linding, G. J. Ostheimer, H. C. Reinhardt, S. E. Ong, C. S. Tan, H. Miao, S. M. Keezer, J. Li, T. Pawson, T. A. Lewis, S. A. Carr, S. J. Smerdon, T. R. Brummelkamp, M. B. Yaffe, A mitotic phosphorylation feedback network connects Cdk1, Plk1, 53BP1, and Chk2 to inactivate the G(2)/M DNA damage checkpoint. *PLoS Biol* **8**, e1000287 (2010).
42. M. Leng, D. W. Chan, H. Luo, C. Zhu, J. Qin, Y. Wang, MPS1-dependent mitotic BLM phosphorylation is important for chromosome stability. *Proc Natl Acad Sci U S A* **103**, 11485-11490 (2006).
43. P. P. Budde, A. Kumagai, W. G. Dunphy, R. Heald, Regulation of Op18 during spindle assembly in Xenopus egg extracts. *J Cell Biol* **153**, 149-158 (2001).
44. H. Li, Y. Wang, X. Liu, Plk1-dependent phosphorylation regulates functions of DNA topoisomerase IIalpha in cell cycle progression. *J Biol Chem* **283**, 6209-6221 (2008).
45. T. Yamaguchi, H. Goto, T. Yokoyama, H. Sillje, A. Hanisch, A. Uldschmid, Y. Takai, T. Oguri, E. A. Nigg, M. Inagaki, Phosphorylation by Cdk1 induces Plk1-mediated vimentin phosphorylation during mitosis. *J Cell Biol* **171**, 431-436 (2005).
46. R. Neef, C. Preisinger, J. Sutcliffe, R. Kopajtich, E. A. Nigg, T. U. Mayer, F. A. Barr, Phosphorylation of mitotic kinesin-like protein 2 by polo-like kinase 1 is required for cytokinesis. *J Cell Biol* **162**, 863-875 (2003).
47. S. Hauf, E. Roitinger, B. Koch, C. M. Dittrich, K. Mechtler, J. M. Peters, Dissociation of cohesin from chromosome arms and loss of arm cohesion during early mitosis depends on phosphorylation of SA2. *PLoS Biol* **3**, e69 (2005).
48. C. Y. Jang, J. A. Coppinger, A. Seki, J. R. Yates, 3rd, G. Fang, Plk1 and Aurora A regulate the depolymerase activity and the cellular localization of Kif2a. *J Cell Sci* **122**, 1334-1341 (2009).
49. L. Macurek, A. Lindqvist, D. Lim, M. A. Lampson, R. Klompmaker, R. Freire, C. Clouin, S. S. Taylor, M. B. Yaffe, R. H. Medema, Polo-like kinase-1 is activated by aurora A to promote checkpoint recovery. *Nature* **455**, 119-123 (2008).